Comparative Mitochondrial Proteomic Analysis of Raji Cells Exposed to Adriamycin

Yu-Jie Jiang,[1] Qing Sun,[2] Xiao-Sheng Fang,[1] and Xin Wang[1]

[1]Department of Hematology, Provincial Hospital affiliated to Shandong University, Jinan, China; [2]Department of Dermatology, Qilu Hospital, Shandong University, Jinan, China

The antitumor mechanisms of adriamycin (ADR) have been thought to contribute to induction of apoptosis and inefficiency of DNA repair, processes that are to a large extent mediated by mitochondria. This study aimed to investigate characteristics of ADR, including its antineoplastic activity, drug resistance, and unexpected toxicity in non-Hodgkin lymphoma (NHL) Raji cells at the mitochondrial proteomic level. The alterations of the mitochondrial proteome of Raji cells treated with ADR were analyzed by two-dimensional differential in-gel electrophoresis (2D-DIGE) coupled with linear ion trap quadrupole–electrospray ionization tandem mass spectrometry (LTQ-ESI-MS/MS). The altered patterns of three identified proteins were validated by Western blot and analyzed by pathway studio software. The results showed that 34 proteins were downregulated and 3 proteins upregulated in the study group compared with the control group. The differentially expressed proteins distributed their functions in reduction-oxidation reactions, DNA repair, cell cycle regulation, transporters and channels, and oxidative phosphorylation. Furthermore, heat shock protein 70 (HSP70), ATP-binding cassette transporter isoform B6 (ABCB6), and prohibitin (PHB) identified in this study may be closely related to chemoresistance and could serve as potential chemotherapeutic targets for NHL. Collectively, these results suggest that specific mitochondrial proteins are uniquely susceptible to alterations in abundance following exposure to ADR and carry implications for the investigation of therapeutic and prognostic markers. Further studies focusing on these identified proteins will be used to predict treatment response and reverse apoptosis resistance, and to explore drug-combination strategies associated with ADR for NHL therapy.
© 2009 The Feinstein Institute for Medical Research, www.feinsteininstitute.org
Online address: http://www.molmed.org
doi: 10.2119/molmed.2008.00129

INTRODUCTION

Chemotherapy is a common method of treatment for non-Hodgkin lymphoma (NHL) and can be effective for varying periods of time. Adriamycin (ADR), a classic anthracycline agent, is widely used in drug combination strategies for NHL therapy, such as cyclophosphamide ± ADR ± vincristine ± prednisolone (CHOP). Some patients have shown resistance to ADR, however, and chemoresistance and the risk of dose-related cardiotoxicity associated with ADR are critical obstacles to successful outcomes (1). Although much progress in conventional therapy for NHL has been achieved during the past decades, 40% to 70% of patients with intermediate- and high-grade NHL fail to achieve long-term disease-free survival, and no curative treatment strategies have been established for patients with low-grade NHL (2,3).

The mechanisms for ADR antineoplastic activity were thought to contribute to the induction of apoptosis and inefficiency of DNA repair (4,5), which were closely mediated by mitochondria (6,7). The mammalian mitochondrial proteome is predicted to comprise of as many as 2000–2500 different proteins (8). Although the mitochondrial proteins and their functional processes have been widely studied (9–11), little is known about mitochondrial proteome alterations of various cells or fractions after exposure to various conditions. Furthermore, although the effects of ADR on NHL have been investigated (12,13), most studies have focused only on evaluating single-protein changes and none on the total cellular proteome or the mitochondrial proteome. We selected Raji cells for study because Raji cells can serve as a model for human lymphomas with mutant p53 and increased BCL2 expression, which are commonly present in patients with NHL and are considered a source of chemotherapy failure in patients whose disease is chemoresistant (14).

Address correspondence and reprint requests to *Xin Wang, Department of Hematology, Provincial Hospital affiliated to Shandong University, No. 324, Jingwu Road, Jinan, 250021, China. Phone: 0086-0531-85186358(B), 0086-13156012606(M); Fax: 0086-0531-87068707(B); E-mail: xinwang55@yahoo.com.cn.*
Submitted January 17, 2009; Accepted for publication February 4, 2009; Epub (www.molmed.org) ahead of print February 5, 2009.

The introduction of proteomics has made it possible to simultaneously analyze changes in multiple proteins. In this study, we performed two-dimensional differential in-gel electrophoresis (2D-DIGE) in combination with linear ion trap quadrupole-electrospray ionization–tandem mass spectrometry (LTQ-ESI-MS/MS) as a nonbiased approach to evaluate mitochondrial proteome alterations in ADR-treated NHL Raji cells. Furthermore, we used Western blot analysis to confirm the expressions of three identified proteins from comparative mitochondrial proteomic analysis and used pathway studio software to further analyze these proteins. We sought to perform a global differential proteome analysis of the mitochondria in Raji cells exposed to ADR.

MATERIALS AND METHODS

Chemicals

The cyanine dyes Cy2, Cy3, and Cy5 and immobilized pH gradient (IPG) strips and 2-DE reagents were purchased from GE Healthcare (Uppsala, Sweden). Protease inhibitor cocktail (cat# p2714), ethylenediaminetetraacetic acid (EDTA), mushroom tyrosinase, most general chemicals for sodium dodecyl sulfate-polyacrylamide gel electrophoresis (SDS-PAGE), buffers, and solutions were purchased from Sigma Chemical Co. (St. Louis, MO, USA) unless otherwise noted. All other general solutions and stocks were prepared using doubly distilled water from a Milli-Q system (Millipore Corp., Bedford, MA, USA). Rabbit anti–cytochrome c oxidase (COX)IV, cathepsin D, proliferating cell nuclear antigen (PCNA), prohibitin (PHB), and β-actin polyclonal antibodies were purchased from Cell Signaling (Danvers, MA, USA). Rabbit-anti–heat shock protein 70 (HSP70) monoclonal antibody was purchased from R&D Systems (Minneapolis, MN, USA). Rabbit anti–ATP-binding cassette transporter isoform B6 (ABCB6) monoclonal antibody was purchased from Abcam (Cambridge, MA, USA).

Cell Culture

The human Burkitt lymphoma Raji cell line was obtained from the Institute of Biochemistry and Cell Biology (SIBS, CAS, Shanghai, China) and was maintained in RPMI-1640 medium (Gibco, Carlsbad, CA, USA) containing 10% heat-inactivated fetal bovine serum albumin (Hangzhou Sijiqing Biological Engineering Materials Co., Ltd., Zhejiang, China), penicillin (100 U/mL), and streptomycin (100 mg/mL) in a 5% CO_2 environment at 37°C. Cells were subcultured every 2 or 3 d. Raji cells were cultured under the same conditions after exposure to ADR.

MTT Analysis

Cell proliferation was evaluated by the MTT [3-(4, 5-dimethylthiazol-2-yl)-2, 5-diphenyl-tetrazolium bromide] assay as described previously (15). The IC50 (half maximal inhibitory concentration) values were determined directly from the semi-logarithmic dose-response curves.

Mitochondria Isolation and Purification Validation

ADR (1.5 μg/mL) was added to 2×10^7 Raji cells at the initiation of the 48-h culture period. The selection of the dose and time of exposure was based on the MTT results. At this stage, the mitochondria of Raji cells were isolated by use of a mitochondrial isolation kit according to the manufacturer's instructions (cat# 89874; Pierce Biotechnology, Rockford, IL, USA). Ensuring that all the steps were performed at 4°C was critical during the isolation process. Separated mitochondria were mounted on glass slides, incubated with 0.1% Janus green B solution for 10 min, and then visualized under a light microscope. Purified mitochondrial pellets were preserved at –80°C until further analysis. The purity of the isolated mitochondria was validated by Western blotting. COXIV, PCNA, and cathepsin D were used as mitochondrial, nuclear, and lysosomal markers, respectively. Briefly, equal amounts of protein samples (20 μg per lane) were separated by 10% SDS-polyacrylamide gel electrophoresis. Immobilized proteins then were transferred to a nitrocellulose membrane, blocked with 5% skim milk in tris-buffered saline tween for 1 h, and subsequently probed with rabbit polyclonal antibodies against COXIV, PCNA, and cathepsin D, respectively, at 4°C overnight. Immunoreactive proteins were visualized by using 1:5000 diluted horseradish peroxidase–linked goat antirabbit antibodies (Dako, Glostrup, Denmark) and enhanced chemiluminescence (GE Healthcare, Milwaukee, WI, USA). Films were scanned and bands quantified by ID Image Analysis Software.

Two-Dimensional Differential In-Gel Electrophoresis and Image Acquisition

Protein concentrations determined by Bio-Rad protein assay for the control and ADR-treated groups were used to normalize the quantities of protein loaded in each sample. Aliquots of 100 μg protein from each of the two samples were individually precipitated at room temperature with methanol and chloroform. Precipitates were solubilized in lysis buffer (7 M urea, 2 M thiourea, 4% CHAPS {3-[(3-cholamidopropyl)-dimethylammonio]-1-propane sulfonate}, 65 mM Tris, 5 mM magnesium acetate) prior to labeling with 200 pmol of either Cy3 (treated) or Cy5 (control). In a similar fashion, 50 μg of each of the two samples were pooled, precipitated, and resuspended in lysis buffer, and incubated for 30 min on ice in the dark, after which the reactions were quenched with the addition of 10 mM lysine (2 μL for each 200 pmol of dye) for 10 min on ice in the dark. Subsamples for each sample (300 μL final volume) were passively rehydrated into 18 cm pH 3-10 (nonlinear) IPG strips for 24 h, followed by simultaneous isoelectric focusing using a Multiphor II (Amersham Biosciences, Uppsala, Sweden) as follows: (a) 30 V, 12 h, step, (b) 500 V, 1 h, gradient, (c) 1000 V, 1 h, gradient, (d) 8000 V, 8 h, gradient, and (e) 500 V, 4 h, step. IPG strips were then transferred onto 12.5%

homogeneous polyacrylamide gels cast with low-fluorescence glass plates using an Ettan-DALT Six system (GE Healthcare, Waukesha, WI, USA). The second-dimension SDS-PAGE was then carried out on two gels simultaneously under standard conditions at 5 W/gel for 30 min followed by a total of 180 W for 4 h with a peltier-cooled DALT II electrophoresis unit (Amersham Biosciences). All of the gels were scanned with the Typhoon 9400 Variable Mode Imager (GE Healthcare) to generate gel images at the appropriate excitation and emission wavelengths from the Cy2-, Cy3-, and Cy5-labeled samples. The resulting gel images were cropped with the ImageQuant software tool and imported into DeCyder 6.5 software. The Biological Variation Analysis module of DeCyder 6.5 was used to compare the control and test samples to generate the list of differentially expressed proteins. Taking a cutoff of 1.5-fold up/downregulation with a *t*-test score $P \leq 0.05$ as an initial threshold for significance, 63 protein spots exhibited statistical significance in the mitochondria of ADR-treated Raji cells. The DeCyder gel-analysis software also generated intimate data and three-dimensional "landscape representations," which enabled us to select spots of interest for further identification. After image acquisition, the gels were subsequently subjected to silver staining.

LTQ-ESI-MS/MS Analysis and Database Searching

A total of 26 protein spots were cut out of 2D-DIGE gels with a Gelpix Spot-Excision Robot (Genetix, Hampshire, UK), and the digested pieces were analyzed via LTQ-ESI-MS/MS (ThermoFinnigan, San Jose, CA, USA) using a surveyor high-performance liquid chromatography system. The system was fitted with a C18 RP column (0.15 mm × 150 mm; Thermo Hypersil-Keystone, Bellefonte, PA, USA). Mobile phase A (0.1% formic acid in water) and mobile phase B (0.1% formic acid in acetonitrile) were used for separation. The tryptic peptide mixtures were eluted using a gradient of 2%–98% B for 60 min. The temperature of the heated capillary was set to 170°C. A voltage of 3.0 kV applied to the ESI needle resulted in a distinct signal. The normalized collision energy was 35%. The number of ions stored in the ion trap was regulated by the automatic gain control. Voltages across the capillary and the quadrupole lenses were tuned by an automated procedure to maximize the signal for the ion of interest. The LTQ mass spectrometer was set so that one full MS scan was followed by 10 MS/MS scans on the 10 most intense ions from the MS spectrum. Dynamic exclusion was set at a repeat count of 2, repeat duration 30 s, and an exclusive duration of 90 s.

For protein identification and statistical validation, the acquired MS/MS spectra were automatically searched against the International Protein Index RAT version 3.15.1 database using the Turbo SEQUEST program in the BioWorks™ 3.1 software suite. An accepted SEQUEST result had to have a DelCN score of at least 0.1 (regardless of charge state). Peptides with a +1 charge state were accepted if they were fully tryptic and had a cross-correlation (Xcorr) of at least 1.9. Peptides with a +2 charge state were accepted if they had an Xcorr ≥2.2. Peptides with a +3 charge state were accepted if they had an Xcorr ≥3.75. Identifications were considered valid when they contained at least two peptide sequences per protein. To sort out a single protein member from a protein group, we chose the protein with the highest sequence coverage.

Validation of Selected Identified Proteins by Western Blotting

To further validate the alterations in protein abundance derived from 2D-DIGE/MS, we examined the variance of three enzymes of interest (HSP70, PHB, and ABCB6) by Western blotting. These proteins were chosen because of their crucial functions in the action of ADR on Raji cells and the commercial availability of the corresponding antibodies. A rabbit polyclonal antibody against human β-actin was used to normalize data to an internal standard. Relative expression levels were evaluated by the optical density ratio.

Identification of Protein Function, Possible Pathways, and Interactions between HSPA9, PHB, and ABCB6

To study functional interactions and possible pathways of the HSP70, PHB, and ABCB6, Pathway Studio 5.0 software (Ariadne Genomics, Rockville, MD, USA) was used. This software helps to interpret biological meaning from gene (protein) expression, build and analyze pathways, and find relationships among genes, proteins, cell processes, and diseases (16). Pathway Studio comes with a built-in resource named ResNet, which is a database of molecular interactions based on natural language processing of scientific abstracts in PubMed. Using ResNet, a researcher can simply drag his favorite gene products onto a new pathway diagram and build a pathway using well-known interactions discussed in existing literature. Briefly, we first imported a protein list including HSP70, PHB, and ABCB6 into a new pathway diagram, and then built a pathway using the option "Find all entities connected to selected entities (Expand Pathway)." The program searches the current pathway database and ResNet for interactions with the selected entities, and adds them to the pathway. After the new pathway was built, we were able to obtain more detailed information for each object by clicking on any of the biological objects.

RESULTS

MTT Assay

NHL Raji cells (4×10^5) were exposed to ADR (0.2, 0.5, 1.0, 1.5, and 2.0 μg/mL) for the various incubation times indicated (24 h, 48 h, and 72 h). The result of the cell proliferation evaluated by the MTT was exhibited as the inhibition rate. Incubation of Raji cells with ADR showed that the inhibition rate varied in a dose- and time-dependent manner. It reached 49.82% with 1.5 μg/mL ADR

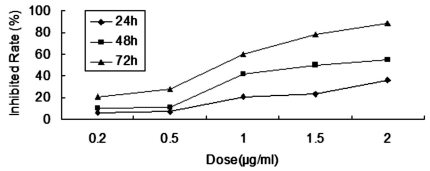

Figure 1. Inhibition of growth rate of Raji cells by ADR administered at various doses and times. NHL Raji cells (4×10^5) were exposed to ADR (0.2, 0.5, 1.0, 1.5, and 2.0 μg/mL) for the various incubation times indicated (24 h, 48 h, and 72 h). Inhibition of growth rate was measured with MTT and reported as a percentage.

treatment for 48 h. On the basis of this result, we used 1.5 μg/mL of ADR for 48 h for further experiments (Figure 1).

Mitochondria Isolation and Purity Validation

To obtain mitochondria of Raji cells with high purity for reliable proteomic analysis, we carried out Janus green B staining to identify the mitochondrial fraction and Western blotting analysis to validate its purity. The isolated mitochondria were stained as bluish green round particles. COXIV was specifically detected in the purified mitochondrial fraction, and this fraction lacked any detectable contamination by abundant nuclear and lysosome proteins such as PCNA and cathepsin D. Our results demonstrated a high purity of mitochondria isolation with the use of our subcellular isolation method (Figure 2).

Physiochemical Characteristics of the Identified Proteins by Comparative Proteomic Analysis

In this study we used 2D-DIGE combined with mass spectrometry and database interrogation to investigate changes in mitochondrial protein abundance of Raji cells exposed to ADR. A total of 1485 spots were detected, and 63 were differentially expressed (≥1.5-fold). We chose 26 spots for further analysis by mass spectrometry and identified 37 unique proteins. Among them, 34 proteins decreased and 3 proteins increased (Figure 3A). The magnitude ratio of changes ranged from 1.93 multiple upregulation (O75947) to 4.71 multiple downregulation (Q9NX63).

A detailed list of total identified proteins, together with their molecular mass, isoelectric point (pI), length, and grand average of hydropathy (GRAVY) were categorized according to their functions (Table 1). The altered proteins identified in this study encompassed a range of mitochondrial functions including oxidative phosphorylation (OXPHOS), cell-cycle regulation, transporters and channels, DNA repair, reduction-oxidation reactions, and protein synthesis and degradation. However, there were still two proteins that had not been matched to their functions (O95897, 027970). The distribution of function, pI, molecular mass, and GRAVY of the identified mitochondrial proteins are shown in Figure 3B. The identified proteins were distributed over a pI range of 4.95–10.57 and a molecular mass range of 13.71–590.99 kDa, indicating that the purification procedure did not cause detectable protein degradation. A relatively large percentage of the proteins had a slightly basic pI value range of 5–9 (32 of 37, 86.49%). No protein with a pI below 4 was detected, indicating that the mitochondrial fractions enriched alkaline proteins, consistent with the results reported by Rezaul *et al*. (17). About 75.68% (28 of 37) proteins identified had masses of 10–60 kDa. The mass of the smallest was 13.71 kDa and the largest was 590.00 kDa. The average pI and molecular mass of the proteins identified were 5.84 and 25.80 kDa, respectively. Furthermore, all proteins with a higher pI did not have a larger molecular mass (for example, GPR81, which has a pI of 9.14 and a molecular mass of only 39.295 kDa). In addition, the symmetric distribution of hydrophobic index (GRAVY) values indicated a range of hydrophobic characteristics in mitochondrial proteins. A cDNA sequence

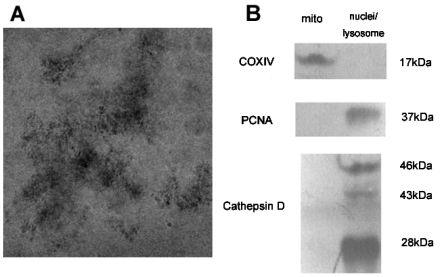

Figure 2. (A) Separated mitochondria were identified by Janus green B staining. The isolated mitochondria were stained as bluish green round particles. (B) Validation of Raji cell mitochondrial purity by Western blotting. An equal amount of proteins (20 μg) were loaded onto a 10% SDS-PAGE with indicated antibodies against marker proteins from mitochondria (mito) and nuclei and lysosomes (nuclei/lysosome). Antibodies against COXIV were used as a marker specific for mitochondria. Antibodies against PCNA and cathepsin D were used as markers for nuclear and lysosome proteins, respectively. The results showed that COXIV was specifically detected in the purified mitochondrial fraction, and this fraction lacked any detectable contamination by abundant nuclear and lysosome proteins such as PCNA and cathepsin D.

(Q6ZWG4), for which no annotation about the protein name or function was well characterized, was present in significantly altered multiples, and it was most likely to be localized in the mitochondria as well. Ten proteins were identified in more than two nonsequential fractions (in either dimension), suggesting that these proteins may have potential posttranslational modifications (18).

Western Blot Analysis of HSP70, PHB, and ABCB6

When we compared mitochondrial lysates from control and ADR-treated Raji cells by Western blotting, we observed that the expressions of HSP70 and PHB were increased whereas the expression of ABCB6 was decreased (Figure 4). The results were in conformity with those obtained with 2D-DIGE.

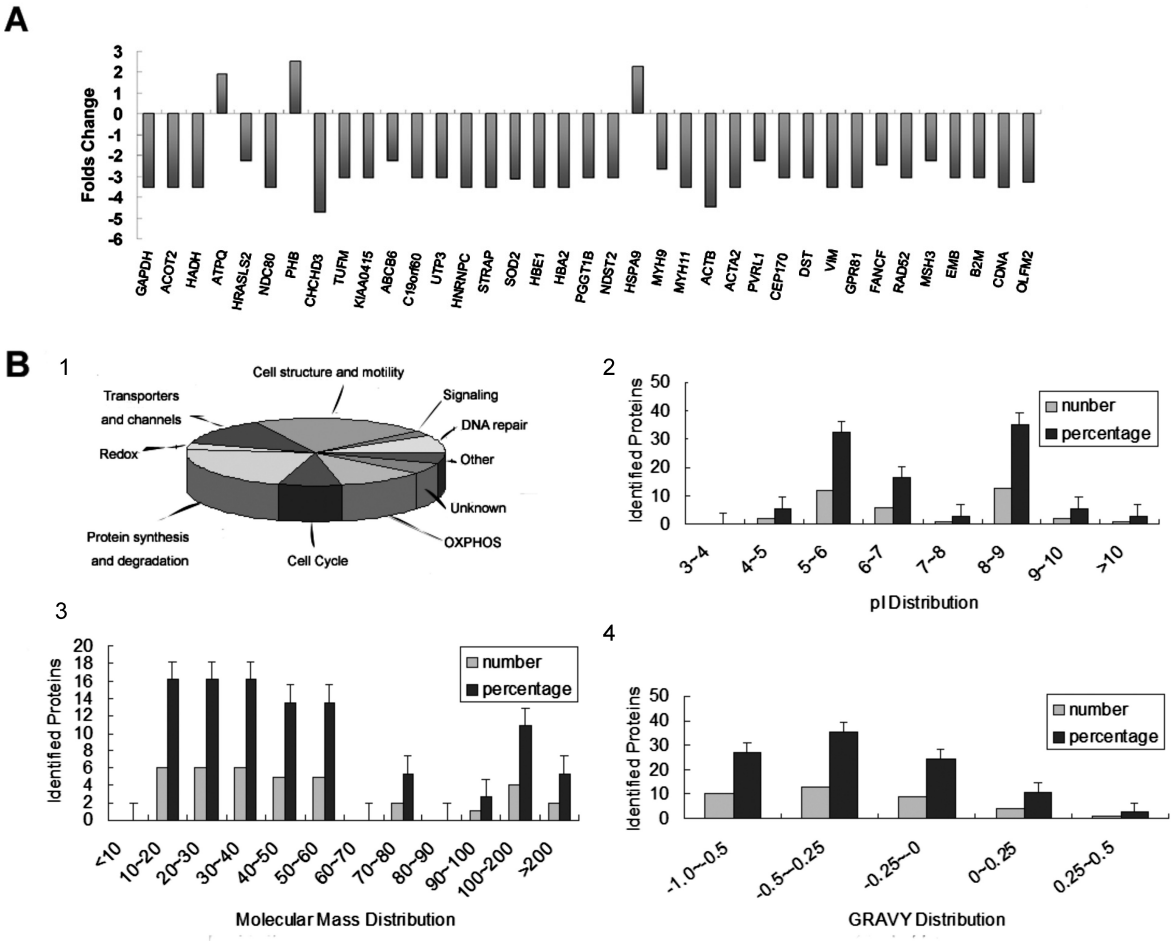

Figure 3. (A) Graphical presentation of altered mitochondrial proteins of Raji cells treated with ADR; 26 spots were analyzed by mass spectrometry and resulted in 37 unique proteins. Among these, 34 proteins decreased and 3 proteins increased. The magnitude ratio of changes ranged from 1.93 multiple upregulation (O75947) and to 4.71 multiple downregulation (Q9NX63). (B) Distribution of function, pI, molecular mass, and GRAVY of the identified mitochondrial proteins; (1) function distribution, (2) pI distribution. (3) molecular mass distribution, (4) GRAVY distribution.

Evaluation of the Bioinformatics Tools

Results of investigations of all identified proteins in several protein databases such as Swiss-Prot, NCBI, EMBL, BioInformatic Harvester, WOLF PROST, Target P, MitoSub, and MitoP2 revealed them to be mitochondria-associated proteins. The pI and molecular mass of each protein were verified based on the 2D-DIGE image. The information obtained from these databases confirmed that our experimental strategy was suitable and unbiased, and also confirmed the sensitivity and specificity of the bioinformatic tools used in combination to predict the presence of mitochondrial proteins.

The software Pathway Studio 5.0 was used to search possible protein-protein interactions, common regulators, cell processes, and related diseases for associations with HSPA9, PHB, and ABCB6. A simplified picture of their interactions is shown in Figure 5. By this approach, we found that proteins belonging to different structural and functional families had PHB as a common target and were involved in processes such as mitogenesis, defense responses, germination, inflammation, proliferation, and apoptosis. Furthermore, most of the diseases associated with these three proteins were cancers derived from various organs (Figure 5).

DISCUSSION

In this study, 2D-DIGE combined with LTQ-ESI-MS/MS was conducted as a nonbiased approach to evaluate mitochondrial proteome alterations in ADR-treated NHL Raji cells. Former studies confirmed that mitochondrial dysfunction is closely related to the pharmacological mechanism of ADR. Therefore, analysis of these differentially expressed mitochondrial proteins may be useful in monitoring the therapeutic response to NHL treatment, especially for investigating the chemoresistance related to the effect of ADR on Raji cells and triaging NHL patients to the best therapy.

Table 1. Identified differentially expressed mitochondrial proteins of Raji cells treated with ADR.

Up- or downregulated proteins	Function group	Protein name (gene name)	Accession no.[a]	Molecular mass	pI	GRAVY	Average ratio
Upregulated							
	OXPHOS						
		ATP synthase d chain, mitochondrial (*ATPQ, ATP5H*)	O75947	18491.21	5.21	−0.554	1.93
	Cell cycle						
		Prohibitin (*PHB*)	P35232	29804.1	5.57	0.024	2.53
	Transporters and channels						
		Heat shock 70 kDa protein 9 precursor (*HSPA9*)	P38646	73680.5	5.87	−0.4	2.29
Downregulated							
	OXPHOS						
		LOC644189 Similar to Acyl-coenzyme A thioesterase 2 (*ACOT2*)	P49753	53237.52	8.82	−0.169	−3.52
		Glyceraldehyde-3-phosphate dehydrogenase (*GAPDH*)	P04406	36053.21	8.57	−0.108	−3.52
		Hydroxyacyl-coenzyme A dehydrogenase, mitochondrial (Precursor) (*HADH*)	Q16836	34277.5	8.88	−0.123	−3.52
	Cell cycle						
		HRAS-like suppressor 2 (*HRASLS2*)	Q9NWW9	18750.4	5.37	−0.029	−2.26
		Kinetochore protein Hec1 (*NDC80*)	O14777	73912.67	5.48	−0.749	−3.52
	Transporters and channels						
		Geranylgeranyl transferase type-1 subunit β (*PGGT1B*)	P53609	42396.3	6.37	−0.265	−3.05
		Isoform 1 of Bifunctional heparan sulfate N-deacetylase/N-sulfotransferase 2 (*NDST2*)	P52849	100874.65	8.81	−0.261	−3.05
		Hemoglobin subunit epsilon (*HBE1*)	P02100	16319.93	8.69	0.027	−3.52
		HBA1 Hemoglobin subunit α (*HBA2*)	P69905	15257.55	8.72	0.048	−3.52
	DNA repair						
		DNA repair protein RAD52 homolog (*RAD52*)	P43351	24539.89	8.43	−0.735	−3.05
		DNA mismatch repair protein Msh3 (*MSH3*)	P20585	127455.94	8.30	−0.327	−2.26
		Similar to Fanconi anemia group F protein (*FANCF*)	Q9NPI8	42254.4	9.11	−0.307	−2.45
	Protein synthesis and degradation						
		Elongation factor Tu, mitochondrial (Precursor) (*TUFM*)	P49411	49541.54	7.26	−0.122	−3.05
		KIAA0415 gene product (*KIAA0415*)	A4D1Z4	164676.62	8.76	−0.080	−3.05
		Isoform 4 of Mitochondrial ATP-binding cassette sub-family B member 6 (*ABCB6*)	Q9NP58	93885.56	8.75	0.149	−2.26
		Isoform 2 of Uncharacterized protein C19orf60 (C19orf60)	Q96EN9	22598.74	6.74	−0.471	−3.05
		Something about silencing protein 10 (*UTP3*)	Q9NQZ2	54557.98	5.5	−1.023	−3.05
		Isoform C1 of Heterogeneous nuclear ribonucleoproteins C1/C2 (*HNRNPC*)	P07910	33670.01	4.95	−0.977	−3.52
		LOC344382 similar to Serine-threonine kinase receptor-associated protein (*STRAP*)	B0AZV0	38438.31	4.98	−0.412	−3.52
		Coiled-coil-helix-coiled-coil-helix domain-containing protein 3 (*CHCHD3*)	Q9NX63	26152.36	8.48	−1.021	−4.71
	Reduction-oxidation reactions						
		Superoxide dismutase (Mn), mitochondrial precursor (SOD2)	P04179	24722.09	8.35	−0.418	−3.12

Continued

Table 1. *Continued.*

Cell structure and motility	Vimentin (*VIM*)	P08670	53651.68	5.06	−0.823	−3.53
	Poliovirus receptor-related protein 1 (Precursor) (*PVRL1*)	Q15223	57158.18	5.77	−0.490	−2.26
	Bullous pemphigoid antigen 1, isoforms 6/9/10 (*DST*)	O94833	590992.91	5.49	−0.674	−3.05
	Centrosomal protein of 170 kDa (*CEP170*)	A6H8 × 9	175292.98	6.64	−0.898	−3.05
	MYH9	P35579	226532.24	5.5	−0.854	−2.67
	MYH11	Q4G140	24976.53	6.54	−0.440	−3.52
	ACTB Actin	P60709	41736.73	5.29	−0.200	−4.44
	ACTA2 Actin	P62736	42008.95	5.24	−0.233	−3.52
Signaling	Probable G-protein coupled receptor 81 (*GPR81*)	Q9BXC0	39295.31	9.14	0.349	−3.52
Other	Embigin precursor (*EMB*)	Q6PCB8	36880.95	6.13	−0.393	−3.05
	B2M β-2-microglobulin (*B2M*)	P61769	13714.57	6.06	−0.376	−3.05
Unknown	Noelin-2 precursor (*OLFM2*)	O95897	51386.34	8.06	−0.309	−3.28
	CDNA FLJ41134 fis, clone BRACE2 (*Q6ZWG4*)	027970	15844.35	10.57	−0.193	−3.52

[a]Accession number refers to Swiss-Prot/TrEMBL database.

Cardiotoxicity

In this study, the protein superoxide dismutase 2 (SOD2, MnSOD), which is involved in reduction-oxidation reactions, was downregulated in Raji cells after exposure to ADR. SOD2 is a major mitochondrial antioxidant that plays a critical role in protecting mitochondria from oxidative damage as a consequence of superoxide generated from the electron transport chain (19). SOD2, peroxiredoxin3, mitochondrial thioredoxin, and mitochondrial thioredoxin reductase have been found to be the main components of the antioxidant system (20–22). Mitochondria are considered a principle source and target of reactive oxygen species (ROS) (23), and the collapse of the mitochondrial transmembrane potential can initiate the signaling cascades involved in apoptosis (24–26). It is well known that the cause of ADR cardiotoxicity is multifactorial, even though most ADR-induced cardiac effects can be attributed to ROS formation, which ultimately results in myocyte apoptosis (2). Abnormal mitochondrial respiration can result in oxidative stress (27), uncoupling of the oxidative pathways from mitochondrial ATP synthesis (28), and subsequent failure of the provision of cellular energy (29). Obviously, the downregulation of SOD2 indicated that the ADR-induced anticancer effect can break down the balance of oxidant and antioxidant in mitochondria. It has been reported that both SOD1 and SOD2 were overexpressed in an ADR-resistant gastric cancer cell line (SGC7901/ADR) (30). Therefore, the identification of novel early biomarkers from drug-induced toxicity could aid drug discovery by improving the toxicity prediction process. Antioxidants such as tocopherol and vigorous exercise before ADR treatment have been used to minimize the cardiotoxic effects of ADR (31,32). How to minimize the cardiotoxic effect but maintain the antitumor effect of ADR, however, remains a formidable question to be solved.

Antineoplastic Activity

Cellular oxidative stress associated with the deficiency of SOD2 in Raji cells after treatment with ADR may induce DNA

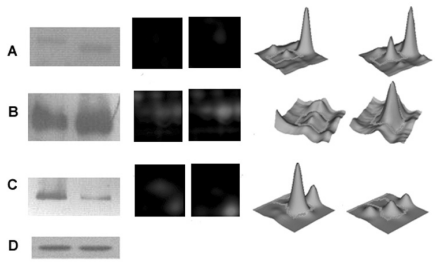

Figure 4. Comparison of HSP 70, PHB, and ABCB6 protein expression levels measured by DIGE and Western blotting. The selected spots were displayed as three-dimensional images and as a partial view of the 2D-DIGE. Verification by Western blotting of HSP70, PHB, and ABCB6 were used to validate the MS results. (A and B) HSP70 (70 kDa) and PHB (32 kDa). Upregulated expression of HSP70 and PHB, respectively. (C) ABCB6 (93 kDa). Downregulated expression of ABCB6. (D) β-actin (43 kDa). β-Actin as an internal marker.

and protein damage, and contribute to chemotherapeutic drug-induced apoptosis in cancer cells (33). In this study, proteins involved in DNA repair, such as Fanconi anemia, complementation group F; mutS homolog 3 (E. coli); and Rad52, were all downregulated in ADR-treated Raji cells. Interestingly, an mRNA sequence (O75947) similar to the ATP synthesis D chain was upregulated, indicating that adequate ATP in mitochondria was necessary for development of apoptosis. This finding is consistent with those reported by Yu *et al.*, who analyzed camptothecin analogue NSC606985-treated acute myeloid leukemic cells (34). In this study, several proteins involved in OXPHOS, including glyceraldehyde-3-phosphate dehydrogenase (GAPDH), hydroxyacyl-coenzyme A dehydrogenase (HADH), and a protein similar to acyl-coenzyme A thioesterase 2 were all downregulated. These results indicated that with the stress of ADR it was necessary to provide sufficient ATP, but the deficiency of some proteins involved in the antioxidant and DNA repair system obstructed normal mitochondrial functions. Thus, cellular proliferation is hindered and apoptosis is an unavoidable event for Raji cells after exposure to ADR.

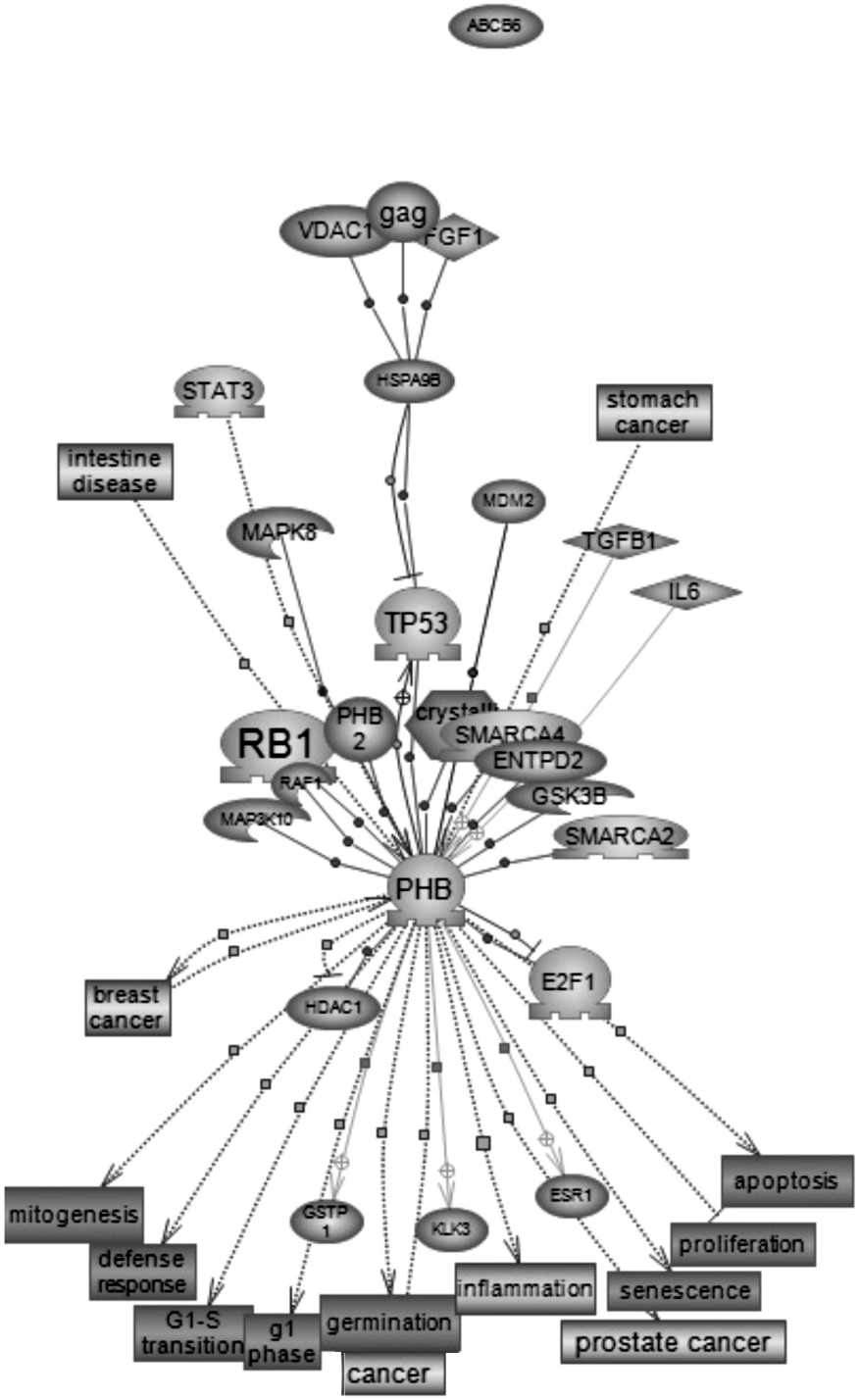

Figure 5. Pathways and networks associated with HSPA9, PHB, and ABCB6. Pathway Studio software was used to map the above three identified proteins onto characterized human pathways and networks that are associated with these proteins based on known protein-to-protein interactions, mRNA expression studies, and other biochemical interactions previously described. Proteins belonging to different structural and functional families had PHB as a common target and were involved in processes such as mitogenesis, defense response, germination, inflammation, proliferation, and apoptosis. Most of the diseases associated with these three proteins were cancer derived from various organs.

Drug Resistance

The 70-kDa protein HSPA9 was significantly upregulated in ADR-treated Raji cells. HSPs are induced as an adaptative response in all cells when they are subjected to various stresses, particularly oxidative stress (35). One member of the HSP family, HSP70, plays a central role in importing mitochondrial protein (36,37). HSP70 protects against oxidative stress by a mitochondrial defense mechanism (38) and may influence both mitochondrial and postmitochondrial apoptotic events, including those associated with members of the Bcl2/Bag/Bax families and the effect of caspases (39). Thus, many investigators believe that the high expression of HSP70 indicates a poor prognosis (35). Kroemer reported that HSP70 could inhibit apoptosis-inducing factor by retaining it in cytoplasm (40). HSP70 is a very effective substance that protects cells from undergoing apoptosis by operating at several levels in the regulation of apoptosis. By treatment with an HSP70-neutralizing peptide, ADD70, Schmitt *et al*. delayed tumor growth and reduced the metastatic potential in mouse melanoma and rat colon carcinoma (41). Furthermore, ADD70 enhanced tumor sensitivity to the cytotoxic drug cisplatin in these cells *in vivo*. Thus, targeting HSP70 is a potential strategy for cancer therapy.

We also found that isoform 4 of mitochondrial ATP-binding cassette subfamily B member 6 (ABCB6) was downregulated. ABCB6 is considered to be localized in the outer mitochondrial membrane as a mitochondrial transporter involved in porphyrin transport (binding heme and porphyrins) (42) and iron homeostasis (43). The downregulation of ABCB6 is consistent with our finding that HBE1 (the hemoglobin subunit epsilon) and HBA2 (HBA1 hemoglobin subunit α) were both downregulated, resulting in deficiency of oxygen transport and subsequent deterioration of the homeostasis of the internal environment (44). Interestingly, ABCB6 is reported to be associated with resistance to cytotoxic agents (45). A study demonstrated that ABCB6-mediated multidrug resistance may be clinically relevant because expression of ABCB6 is increased in hepatocellular cancer (46). Former studies showed that there are many mechanisms of chemoresistance to anthracyclines and that resistance is often multifractional. We presumed that owing to various cell lines, tissues, or drugs, the expression of proteins and their involvement in multidrug resistance are diverse. More investigations are required to validate this hypothesis.

Notably, PHB, which might be involved in chemoresistance, was demonstrated to be upregulated in ADR-treated Raji cells. PHB is a highly conserved mitochondrial protein that is thought to play roles in cell-cycle control, differentiation, senescence, and antiproliferative activity (47). Former studies confirmed that PHB may defend against oxidant injury, suppress apoptosis in mammalian cells, and promote survival of cancer cells (48,49). Results of a study by Fusaro *et al*. indicated that overexpression of PHB in a human lymphoma cell line blocked apoptosis induced by the topoisomerase I inhibitor camptothecin (50). Reportedly, PHBs function as negative regulators of E2F-mediated transcription (51). The E2F transcription factors play a major role in regulating the proliferation, differentiation, and apoptosis of mammalian cells. The transcriptional activity of the E2Fs is modulated mainly by the Rb family of proteins, and PHB interacts with Rb family members to repress E2F transcriptional activity (50). The correlation of PHB, E2F, and Rb can also be found in our pathway analysis, as shown in Figure 6. Novel approaches that target PHB may lead to the development of new therapies that limit the development of resistance or enhance the sensitivity of lymphoma cells to ADR.

It is well known that the lack of a complete and long-lasting response to chemotherapy is a main drawback limiting the clinical potential of ADR in NHL treatment. Proteomic techniques have identified novel biomarkers with the potential to enable prediction of response to anticancer therapy, particularly chemoresistance. Before these "potential prognostic markers" are applied clinically, however, further studies are required to validate whether these alterations are the cause or the result of resistance to anticancer therapy.

In conclusion, we used 2D-DIGE in combination with ESI-MS/MS to analyze the changes in mitochondrial protein expression in control Raji and ADR-treated Raji cells and identified several biomarkers with the potential to enable prediction of response to anticancer therapy. Defects in the mitochondrial antioxidant defense system, DNA repair, and OXPHOS might be the main mechanisms involved in the effect of ADR on the mitochondria of Raji cells. Defects in the mitochondrial antioxidant defense system have dual effects on the anticancer mechanism and cardiac toxicity. We also found a series of proteins associated with chemoresistance relevant to ADR, including HSP70, PHB, and ABCB6. However, such markers require functional studies before clinical use. Further direct analysis on these identified proteins may provide potential prognostic markers and facilitate exploration of drug-combination strategies to avoid unexpected toxicity associated with ADR for NHL treatment.

ACKNOWLEDGMENTS

This study was supported by: Natural Science Foundation of Shandong Province, China (No. 2007C053); Project of Scientific and Technological Development of Shandong Province, China (N2007GG10). We also thank the staff of Central Laboratory of Provincial Hospital affiliated to Shandong University and J Hu (Shanghai Applied Protein Technology Co. Ltd).

DISCLOSURE

We declare that the authors have no competing interests as defined by *Molecular Medicine*, or other interests that might be perceived to influence the results and discussion reported in this paper.

REFERENCES

1. Multani P, White CA, Grillo-Lopez A. (2001) Non-Hodgkin's lymphoma: review of conventional treatments. *Curr. Pharm. Biotechnol.*. 2:279–91.
2. Armitage JO. (1993) Treatment of non-Hodgkin's lymphoma. *N. Engl. J. Med.*. 328:1023–30.
3. Parker SL, Tong T, Bolden S, Wingo PA. (1997) Cancer statistics. *CA Cancer. J. Clin.* 47:5–27.
4. Patel S, Sprung AU, Keller BA, Heaton VJ, Fisher LM. (1997) Identification of yeast DNA topoisomerase II mutants resistant to the antitumor drug doxorubicin: implications for the mechanisms of doxorubicin action and cytotoxicity. *Mol. Pharmacol.* 52:658–66.
5. Singh V, Singh SM. (2007) Effect of high cell density on the growth properties of tumor cells: a role in tumor cytotoxicity of chemotherapeutic drugs. *Anticancer Drugs* 18:1123–32.
6. Gunter TE, Gunter KK, Sheu SS, Gavin CE. (1994) Mitochondrial calcium transport: physiological and pathological relevance. *Am. J. Physiol.* 267:C313–39.
7. Gunter TE, Buntinas L, Sparagna GC, Gunter KK. (1998) The Ca2+ transport mechanisms of mitochondria and Ca2+ uptake from physiological-type Ca2+ transients. *Biochim. Biophys. Acta* 1366:5–15.
8. Goffart S, Martinsson P, Malka F, Rojo M, Spelbrink JN. (2007) The mitochondria of cultured mammalian cells; II: expression and visualization of exogenous proteins in fixed and live cells. *Methods Mol. Biol.* 372:17–32.
9. Rorbach J, Soleimanpour-Lichaei R, Lightowlers RN, Chrzanowska-Lightowlers ZM. (2007) How do mammalian mitochondria synthesize proteins? *Biochem. Soc. Trans.* 35:1290–1.
10. de Cavanagh EM, Inserra F, Ferder M, Ferder L. (2007) From mitochondria to disease: role of the renin-angiotensin system. *Am. J. Nephrol.* 27:545–53.
11. Schleicher E, Friess U. (2007) Oxidative stress, AGE, and atherosclerosis. *Kidney Int. Suppl.* S17–26.
12. Huang MQ, *et al.* (2007) In vivo monitoring response to chemotherapy of human diffuse large B-cell lymphoma xenografts in SCID mice by 1H and 31P MRS. *Acad. Radiol.* 14:1531–9.
13. Vaisheva F, Delbes G, Hales BF, Robaire B. (2007) Effects of the chemotherapeutic agents for non-Hodgkin lymphoma, cyclophosphamide, doxorubicin, vincristine, and prednisone (CHOP), on the male rat reproductive system and progeny outcome. *J. Androl.* 28:578–87.
14. Wilson WH, *et al.* (1997) Relationship of p53, bcl-2, and tumor proliferation to clinical drug resistance in non-Hodgkin's lymphomas. *Blood.* 89:601–9.
15. Litvinova E, Gurova K, Chimishkian K, Mentkevich G. (1999) Effects of CSFS and their combinations with chemotherapeutic agents (CH) on leukemic blasts (LB) in children (MTT-assay). *Adv. Exp. Med. Biol.* 457:585–92.
16. Nikitin A, Egorov S, Daraselia N, Mazo I. (2003) Pathway studio—the analysis and navigation of molecular networks. *Bioinformatics* 19:2155–7.
17. Rezaul K, Wu L, Mayya V, Hwang SI, Han D. (2005) A systematic characterization of mitochondrial proteome from human T leukemia cells. *Mol. Cell. Proteomics* 4:169–81.
18. Zhu K, Zhao J, Lubman DM, Miller FR, Barder TJ. (2005) Protein pI shifts due to posttranslational modifications in the separation and characterization of proteins. *Anal. Chem.* 77:2745–55.
19. Lee YH, Boelsterli UA, Lin Q, Chung MC. (2008) Proteomics profiling of hepatic mitochondria in heterozygous Sod2+/- mice, an animal model of discreet mitochondrial oxidative stress. *Proteomics* 8:555–68.
20. Hoye AT, Davoren JE, Wipf P, Fink MP, Kagan VE. (2008) Targeting mitochondria. *Acc. Chem. Res.* 41:87–97.
21. Ishii N. (2007) Role of oxidative stress from mitochondria on aging and cancer. *Cornea* 26:S3–9.
22. Orrenius S. (2007) Reactive oxygen species in mitochondria-mediated cell death. *Drug Metab. Rev.* 39:443–55.
23. Major T, von Janowsky B, Ruppert T, Mogk A, Voos W. (2006) Proteomic analysis of mitochondrial protein turnover: identification of novel substrate proteins of the matrix protease pim1. *Mol. Cell. Biol.* 26:762–76.
24. Green DR, Reed JC. (1998) Mitochondria and apoptosis. *Science* 281:1309–12.
25. Bernardi P, Scorrano L, Colonna R, Petronilli V, Di Lisa F. (1999) Mitochondria and cell death. Mechanistic aspects and methodological issues. *Eur. J. Biochem.* 264:687–701.
26. Susin SA, *et al.* (1999) Molecular characterization of mitochondrial apoptosis-inducing factor. *Nature* 397:441–6.
27. Nemoto S, Takeda K, Yu ZX, Ferrans VJ, Finkel T. (2000) Role for mitochondrial oxidants as regulators of cellular metabolism. *Mol. Cell. Biol.* 20:7311–8.
28. Beltran B, *et al.* (2002) Inhibition of mitochondrial respiration by endogenous nitric oxide: a critical step in Fas signaling. *Proc. Natl. Acad. Sci. U. S. A.* 99:8892–7.
29. Douette P, Sluse FE. (2006) Mitochondrial uncoupling proteins: new insights from functional and proteomic studies. *Free Radic. Biol. Med.*. 40:1097–107.
30. Yang YX, Hu HD, Zhang DZ, Ren H. (2007) Identification of proteins responsible for the development of adriamycin resistance in human gastric cancer cells using comparative proteomics analysis. *J. Biochem. Mol. Biol.* 40:853–60.
31. Kim SY, *et al.* (2006) Doxorubicin-induced reactive oxygen species generation and intracellular Ca2+ increase are reciprocally modulated in rat cardiomyocytes. *Exp. Mol. Med.* 38:535–45.
32. Wonders KY, Hydock DS, Schneider CM, Hayward R. (2008) Acute exercise protects against doxorubicin cardiotoxicity. *Integr. Cancer Ther.* 7:147–54.
33. Chandra J, Samali A, Orrenius S. (2000) Triggering and modulation of apoptosis by oxidative stress. *Free Radic. Biol. Med.*. 29:323–33.
34. Yu Y, *et al.* (2007) Subcellular proteome analysis of camptothecin analogue NSC606985-treated acute myeloid leukemic cells. *J. Proteome Res.* 6:3808–18.
35. Ciocca DR, Calderwood SK. (2005) Heat shock proteins in cancer: diagnostic, prognostic, predictive, and treatment implications. *Cell Stress Chaperones*. 10:86–103.
36. Mizzen LA, Kabiling AN, Welch WJ. (1991) The two mammalian mitochondrial stress proteins, grp 75 and hsp 58, transiently interact with newly synthesized mitochondrial proteins. *Cell Regul.* 2:165–79.
37. Voos W, Rottgers K. (2002) Molecular chaperones as essential mediators of mitochondrial biogenesis. *Biochim. Biophys. Acta* 1592:51–62.
38. Werninghaus K, Handjani RM, Gilchrest BA. (1991) Protective effect of alpha-tocopherol in carrier liposomes on ultraviolet-mediated human epidermal cell damage in vitro. *Photodermatol. Photoimmunol. Photomed.* 8:236–42.
39. Samali A, Orrenius S. (1998) Heat shock proteins: regulators of stress response and apoptosis. *Cell Stress Chaperones* 3:228–36.
40. Perry ME, Dang CV, Hockenbery D, Moll U. (2004) Highlights of the National Cancer Institute Workshop on mitochondrial function and cancer. *Cancer Res.* 64:7640–4.
41. Schmitt E, *et al.* (2006) Heat shock protein 70 neutralization exerts potent antitumor effects in animal models of colon cancer and melanoma. *Cancer Res.* 66:4191–7.
42. Krishnamurthy PC, *et al.* (2006) Identification of a mammalian mitochondrial porphyrin transporter. *Nature* 443:586–9.
43. Mitsuhashi N, *et al.* (2000) MTABC3, a novel mitochondrial ATP-binding cassette protein involved in iron homeostasis. *J. Biol. Chem.* 275:17536–40.
44. Desmard M, Boczkowski J, Poderoso J, Motterlini R. (2007) Mitochondrial and cellular heme-dependent proteins as targets for the bioactive function of the heme oxygenase/carbon monoxide system. *Antioxid. Redox. Signal* 9:2139–55.
45. Szakacs G, *et al.* (2004) Predicting drug sensitivity and resistance: profiling ABC transporter genes in cancer cells. *Cancer Cell* 6:129–37.
46. Emadi-Konjin HP, *et al.* (2002) Isolation of a genomic clone containing the promoter region of the human ATP binding cassette (ABC) transporter, ABCB6. *Biochim. Biophys. Acta* 1574:117–30.
47. Chen JC, Jiang CZ, Reid MS. (2005) Silencing a prohibitin alters plant development and senescence. *Plant J.* 44:16–24.
48. Theiss AL, *et al.* (2007) Prohibitin protects against oxidative stress in intestinal epithelial cells. *FASEB J.* 21:197–206.
49. Chowdhury I, *et al.* (2007) Apoptosis of rat granulosa cells after staurosporine and serum withdrawal is suppressed by adenovirus-directed overexpression of prohibitin. *Endocrinology* 148:206–17.
50. Fusaro G, Wang S, Chellappan S. (2002) Differential regulation of Rb family proteins and prohibitin during camptothecin-induced apoptosis. *Oncogene* 21:4539–48.
51. Choi D, Lee SJ, Hong S, Kim IH, Kang S. (2008) Prohibitin interacts with RNF2 and regulates E2F1 function via dual pathways. *Oncogene* 27:1716–25.